ELSEVIER

Polymer 41 (2000) 5327–5338

polymer

Coherence of thermal transitions in poly(*N*-vinyl pyrrolidone)–poly(ethylene glycol) compatible blends 1. Interrelations among the temperatures of melting, maximum cold crystallization rate and glass transition

M.M. Feldstein*, G.A. Shandryuk, S.A. Kuptsov, N.A. Platé

A.V. Topchiev Institute for Petrochemical Synthesis, Russian Academy of Sciences, 29 Leninsky prospekt, 117912, Moscow, Russian Federation

Received 3 August 1999; received in revised form 25 September 1999; accepted 15 October 1999

Abstract

The phase behaviour of blends of high-molecular weight poly(*N*-vinyl pyrrolidone) (PVP) with short-chain poly(ethylene glycol) (PEG) of $M_w = 400$, prepared by drying their solutions in a common solvent (ethyl alcohol), was studied using DSC. Upon heating of cool-quenched samples a single glass transition was observed, followed by an exotherm corresponding to cold crystallization of excess PEG, a melting endotherm, and an endotherm corresponding to vaporization of absorbed water. The temperatures of glass transition (T_g), PEG cold crystallization (T_c), and melting (T_m), along with the change in heat capacity (ΔC_p) between the polymer's glassy and rubbery states at T_g, vary with blend composition and hydration. As a result the T_g/T_m, T_c/T_m and T_c/T_g ratios for PVP–PEG blends are functions of composition. PVP–PEG compatibility is due to H-bonding of PEG terminal hydroxyls to the carbonyls in the PVP repeating units. Large negative deviations of T_g values from the calculated weight averages, found mainly for PVP-overloaded blends, signify strong PVP–PEG interaction and free volume formation.

Keywords: Poly(*N*-vinyl pyrrolidone); Poly(ethylene glycol); Compatibility

1. Introduction

Differential scanning calorimetry (DSC) thermograms, which plot heat capacity, C_p, versus temperature, provide a highly informative tool to study the phase behaviour of polymers. A range of important thermodynamic characteristics may be readily determined from DSC traces. Such characteristics are glass transition temperature (T_g), change in heat capacity at T_g (ΔC_p), heat and temperature of melting (ΔH_m, T_m), and enthalpy and temperature of polymer crystallization (ΔH_c, T_c). For hydrophilic polymers containing water, taken up from the environment via vapour state or residual from material processing, the temperature and heat of water thermodesorption along with a content of sorbed water can also be measured on DSC heating scans.

A number of empirical rules have been established regarding the transition temperatures for various homopolymers [1–4]. Boyer [2] and Beamen [3] have demonstrated a linear correlation between T_m and T_g, with slope and intercept related to chemical structure. Boyer classified polymers into two large groups as symmetrical (sterically nonrestricted, low cohesive energy density (CED) macromolecules with flexible chains) and unsymmetrical (sterically restricted, substituted polymers with stiff backbone and bulky side groups). However, in an extensive study of 132 polymers, subsequent investigations found no sharp division between the T_g/T_m ratios observed for symmetrical and unsymmetrical polymers. Thus T_g/T_m (in K) quantity has been reported to range from 0.5 to 0.8 with an average value to be [1]:

$$\frac{T_g}{T_m} = 0.666 \tag{1}$$

Moreover, this rule was also shown to be true for both organic and inorganic compounds [5].

Similarly, the ratio T_c/T_m (where T_c designates the temperature of maximum crystallization rate upon polymer cooling from melt) shows an almost constant value for a wide variety of metals, organic and inorganic substances, varying between 0.75 and 0.90. According to the Mandelkern's rule [6], the rate of polymer crystallization

* Corresponding author. Fax: +7-095-230-2224.
E-mail address: mfeld@ips.ac.ru (M.M. Feldstein).

0032-3861/00/$ - see front matter
PII: S0032-3861(99)00802-2

is maximum at a temperature of about 0.9 of the melting point. Closer examination for polymers has found [7]:

$$\frac{T_c}{T_m} = 0.82 - 0.83 \tag{2}$$

In addition, the T_c relates to T_g by the equation [1,8,9]:

$$\frac{T_c}{T_g} = 1.20 - 1.33 \tag{3}$$

Following Boyer [2], the minimum temperature required for crystallization, T_c (°C), is also a function of T_g. For a wide range of polymers, the points fall on a straight line, defined by the equation:

$$T_c\,(°C) = 32.5 + 1.125\,T_g(°C) \tag{4}$$

More general empirical relations between T_g, T_m and T_c include consideration of all three transition temperatures [5]:

$$T_c = \frac{(T_g + T_m)}{2} \quad \text{or} \quad T_c - T_g = T_m - T_c \tag{5}$$

Although the rules (1)–(5) are totally empirical, they invoke fundamental structure–property relationships, which have begun only recently to find quantitative comprehension. The T_g is defined as a function of coordination number, z, and total interaction energy, $\langle Do\rangle$, of the atoms forming the polymer segment [10]:

$$T_g = 0.445\frac{z\langle Do\rangle}{R} \tag{6}$$

where R is the universal gas constant. Since z is in inverse proportion to free volume (Eq. (6)) outlines the energy–volume ratio, related to CED. This definition of T_g is in agreement with the results of recent work [11], dealing with the calculations of T_g values for the series of aliphatic acrylate and methacrylate polymers on the basis of energy–volume–mass (EVM) model.

Like T_g, the melting points of polymers are greater the greater the CED, and the greater the chain stiffness, i.e. the smaller the free volume [2]. The physical meaning of the constancy of the T_g/T_m ratio (1) is that the molecular packing coefficients of crystalline polymers at T_m approximate those of amorphous polymers at T_g, that is the fusion of polymer crystals and transition of amorphous polymer glasses into viscoelastic state occurs upon achieving the same values of the fraction of full free volume [12], equal to $1 - (T_g/T_m) = 1 - 0.666 = 0.333$.

Based on an iso-volume state model and a crystallization theory, the relationships between T_m, T_c and T_g are formulated by Okui [1] as follows:

$$\frac{T_g}{T_m} = \frac{C - (\alpha_c/\alpha_g)}{C + 1}, \tag{7}$$

$$\frac{T_c}{T_m} = \frac{C}{C + 1}, \tag{8}$$

$$\frac{T_m - T_c}{T_c - T_g} = \frac{\alpha_g}{\alpha_c}, \tag{9}$$

$$C = \sqrt{1 + (\Delta E/K)} \tag{10}$$

where α_g, α_c are the thermal expansion coefficients of glassy and crystalline polymers, respectively; ΔE is an activation energy for polymer segment migration through the nucleus–melt interface and K is the nucleation parameter associated with the mean surface energy, δ, and the heat of fusion, ΔH_m:

$$K = \frac{n\delta^2}{\Delta H_m}, \qquad \delta = \sqrt{h_0\sigma_e\sigma_m} \tag{11}$$

In Eq. (11), n is a nucleation mode parameter, h_0 the thickness of the depositing growth layer, and σ_e and σ_m the end and the lateral surface energies, respectively. In general, C varies from 3 to 9 with a mean value of about 5. The average $\Delta E/K$ magnitude is around 23 for most polymers [1].

ΔE may be compared with the activation energy for viscous flow or self-diffusion of macromolecular segments, which are the characteristics of chain mobility. ΔH_m is a measure of intermolecular forces and δ affects the degree of polymer crystallinity [1]. All three parameters may be expressed in terms of cohesive energy, chain stiffness and geometry, which contribute to the free volume. Both T_g and T_m are shown to invoke the same fundamental properties of polymers [2,10–12].

The numerical quantities outlined by Eqs. (1)–(5) and (7)–(9), hold only for individual homopolymers and, in general, are inapplicable for copolymers or polymer blends [10,12]. The view taken in this series of papers is that a blend of compatible polymers can behave like an individual homopolymer, demonstrating the compositional dependence of the quantities defined by Eqs. (1)–(10). In this work, we follow terminology defined by Paul and Newman [13]: a blend is considered compatible if mixed polymers are capable to exhibit a total miscibility on a molecular scale. Miscibility on the molecular scale is not necessarily random within the entire range of composition and temperatures: interactions between similar or different macromolecules may lead to a certain amount of clustering or other nonrandom arrangement of polymer segments. Thus, the crystallization of polymer in the blend is not treated as a sign of incompatibility if the crystallizable polymer remains at least partially amorphous and miscible with the other component in the amorphous state below T_m [13].

In many blend systems, a homogeneous phase is obtained because of the existence of specific favourable interactions between different polymer components, which allow mixing on a molecular scale. One such favourable interaction is H-bonding that has been reported for many polymer blends [14–17]. Polymers containing ternary amide groups, such as poly(*N*-vinyl pyrrolidone) (PVP), are potentially good proton acceptors due to the basic nature of the functional groups [18]. In a similar way, another good proton-accepting

polymer is poly(ethylene oxide) (PEO) [19], and therefore it comes as no surprise that PVP and PEO are reported to form only incompatible binary blends [20], while in ternary blends with such proton-donating compatibilizers as poly(acrylic acid) and poly(methacrylic acid) they display compatibility [17]. As the more potent competitor in H-bonding with polyacids, in doing so the PVP supersedes PEO in forming hydrogen-complex with the proton-donating polymer [21].

In contrast to high molecular weight PEO, short-chain poly(ethylene glycol) represents a symmetric telechelic polymer with controlled molecular weight and narrow molecular weight distribution, carrying two proton-donating hydroxyl groups at the chain ends. The term "PEG" is used in this work to define the oligomeric starting polymers containing terminal hydroxyls, while the "PEO" is employed to emphasize that the contribution of end-chain hydroxyls to miscibility is considered to be negligible due to higher molecular weight and lower end-group concentration. PVP compatibility with short-chain PEG follows directly from the well-known observation of unlimited PVP solubility in liquid PEG [22]. In this way, the PVP–PEG compatible blends may be treated as the solutions of high molecular weight PVP in liquid oligo(ethylene glycol).

PVP–PEG compatibility in blends has been determined by FTIR spectroscopy to be due to H-bonded interactions between the hydrogen atom of PEG terminal groups and electronegative oxygen atom in the carbonyl groups of the monomer units of the comparatively longer PVP chains [23,24]. High molecular weight PVP forms compatible blends only with short-chain PEGs [25], ranging in molecular weight from 200 to 600 g mol^{-1}. PEGs of higher molecular weight are miscible with amorphous PVP in the melt, but these do not form homogeneous amorphous mixture with PVP below T_m. This is indicative of PVP incompatibility with long-chain PEG and PEO on the molecular scale, that is shown by direct optical microinterference measurement of PVP–PEG spontaneous mixing [26], and confirmed with DSC and wide angle X-ray scattering (WAXS) [27]. Microphase separation in PVP blends with PEO ($M_w = 32\,000$) has been also demonstrated by Cesteros et al. [20] with DSC and DMTA. These findings are explicable, because with the rise in PEG molecular weight the end-group contribution to compatibility becomes negligible.

H-bonding of PEG terminal hydroxyls to carbonyls in the PVP repeat units results in a high degree of the orientation of the PEG macromolecules with respect to longer PVP chains, as has been established with WAXS and rheological techniques [23,28]. The PVP–PEG complex is akin to those formed by H-bonds between the units of polar polymers and complementary end-groups of a range of oligomers, such as phenolic surfactants [29,30], but the former is distinguishable by its capability to form simultaneously two strong H-bonds through both PEG terminal groups. The mechanism of PVP–PEG H-bonding implies the cross-linking of PVP macromolecules by relatively long and flexible PEG chains. The resulting network structure of PVP–PEG complex reveals a range of unique physical properties, including a high elasticity, similar to that of lightly cross-linked rubbers [23,31], and pressure-sensitive character of adhesion toward various substrates [32–34]. With conventional compounding methods, polymer blends, which possess high tack, do so because their parent polymers are also tacky. This is not the case for the present PVP–PEG adhesive, where adhesion has been found to arise within a narrow range of PEG concentration [32]. Tailoring adhesive properties by blending two non-adhesive polymers, PVP and PEG, provides an indirect evidence of their compatibility and the formation of new, distinguishable and independent supramolecular species. Indeed, the PVP–PEG blends have been defined as a complex of stoichiometric composition, in which approximately 30% of PVP repeat units are bonded to PEG terminal hydroxyls and nearly 15 PEG chains are associated on average with 100 PVP units [28].

This present series of papers report on the phase behaviour of the PVP–PEG blends as examined by DSC of cool-quenched samples under heating. In contrast to T_c definition given above, the T_c is here defined as the temperature at which the rate of crystallization is maximum and coincides with a peak temperature of cold crystallization under heating through T_g of a blend, produced by quench-cooling from the melt. The first paper considers the correlation between temperatures of glass transition, PEG cold crystallization and melting. The second paper presents the thermodynamic analysis of T_c dependence on T_g. The third paper describes the impact of sorbed water upon relaxation and phase transitions.

2. Experimental

PVP (Kollidon K-90), $M_w = 1\,000\,000$ g mol^{-1}, and PEG (Lutrol E-400), $M_w = 400$ g mol^{-1}, were obtained from BASF and used as-received. Both polymers are hygroscopic and the degree of their hydration, evaluated by the weight loss under drying at 105°C, is taken into account to prepare physical blends spanning the entire range of compositions. Depending on the relative humidity (RH) of the surrounding atmosphere, PVP hydration ranged from 6 to 8 wt%, while the PEG contained less sorbed water (0–1 wt%).

The blends, referred throughout this work as "fresh", were produced by dissolving PVP and PEG in common solvent (ethyl alcohol) followed by the solvent evaporation at ambient temperature and RH until a constant weight was attained. Solvent removal was verified by FTIR spectroscopy, observing the lack of methylene group stretching vibrations at 2974 and 1378 cm^{-1} in the IR spectrum. The hydration of freshly prepared PVP–PEG blends averaged

Table 1
Effects of scanning rate on the temperatures and heats of phase transitions in PVP–PEG blends

PEG content (wt%)	0	36	53	66	69	71	85	92	100
T_g (°C) (20°C min^{-1})	176.9	−46.6	−54.8	−60.0	−63.6	−63.0	−65.7	−64.7	−72.3
T_g (°C) (0°C min^{-1})	174.0	−57.27	−59.75	−64.05	−65.95	−66.20	−68.23	−71.0	−73.4
R	0.987	0.997	0.995	0.967	0.973	0.972	0.989	0.978	0.945
P	0.0003	0.005	0.005	0.033	0.027	0.028	0.010	0.021	0.055
T_c (°C) (20°C min^{-1})				−31.0	−42.0	−43.4	−48.1	−50.2	
T_c (°C) (0°C min^{-1})				−39.65	−49.55	−50.65	−53.0	−54.8	
R				0.912	0.969	0.986	0.814	0.989	
P				0.081	0.030	0.014	0.186	0.011	
T_m (°C) (20°C min^{-1})				6.1	3.9	5.6	5.3	5.4	5.7
T_m (°C) (0°C min^{-1})				5.75	2.4	5.10	5.05	4.55	5.25
R				0.424	0.895	0.863	0.788	0.599	0.689
P				0.570	0.105	0.137	0.212	0.404	0.311
T_d (°C) (20°C min^{-1})	108.7				120.4		136.4		
T_d (°C) (0°C min^{-1})	82.48				108.75		104.00		
R	0.941				0.960		0.963		
P	0.017				0.040		0.037		
ΔH_c (J g^{-1}) (20°C min^{-1})				36.2	37.0	50.7	37.1		
ΔH_c (J g^{-1}) (0°C min^{-1})				36.60	44.35	52.35	46.1		
R				0.756	0.976	0.700	0.995		
P				0.243	0.024	0.304	0.005		
ΔH_m (J g^{-1}) (20°C min^{-1})				36.9	37.9	54.1	37.5		118.1
ΔH_m (J g^{-1}) (0°C min^{-1})				44.05	47.05	66.70	41.05		109.6
R				0.850	0.969	0.994	0.959		0.045
P				0.150	0.030	0.006	0.040		0.955

7.2 ± 2.2 wt%. From this point on the term "hydrogels" is used to designate equilibrium hydrated PVP–PEG blends.

Since our earlier obtained data on PVP–PEG H-bonding [24] and water vapour sorption [35] provide grounds for considering sorbed water as the third component of the PVP–PEG complex, our concern here is confined mainly at the DSC study of PVP–PEG hydrogel phase behaviour. However, being a common solvent for both PVP and PEG, water is supposed to serve as a compatibilizer in PVP–PEG blends. To test this hypothesis, so-called "dry" blends were prepared by drying hydrogels at 105°C until termination of weight loss. Strictly speaking, efforts to prepare perfectly anhydrous samples were unsuccessful because, due to the high affinity for water vapour, dry samples contained 0.7 ± 0.2 wt% of moisture sorbed in the course of sample handling and weighing. Dry blends were stored until use over P_2O_5, while hydrogels were either exposed to atmospheric humidity or equilibrated in a desiccator over aqueous H_2SO_4 solution of controlled density (1.335 g cm^{-3}) which maintained the required RH = 50%.

The samples of PVP–PEG blends were subjected to several different DSC experiments to assess the effects of various test procedures (heating rates) and storage conditions (time and RH) on the transition temperatures and enthalpy changes occurring in each system. Approximately 5–15 mg samples of each composition were sealed in standard aluminium pans with lids pierced with a sharp pin to enable the evaporation of sorbed water. The samples were analysed under a dry argon purge (50 ml min^{-1}) in a Mettler TA 4000/DSC 30 DSC, calibrated for temperature and heat flow using indium and gallium ultrapure standards. All reported values are the average of replicate experiments varying less than 1–2%. All the samples were reweighed after scanning and weight loss was registered.

In the DSC apparatus, samples were first cooled with liquid nitrogen from ambient temperature to −100°C over 2–3 min and then heated at a rate of 20°C min^{-1} (unless otherwise specified) to 200°C. Upon heating, a heat capacity jump followed by single exotherm coupled with symmetric endotherm, and high-temperature endotherms were normally observed for PVP–PEG blends. These four transitions were, respectively, attributed to the glass transition, PEG cold crystallization, melting, and water thermodesorption, as explained in the following section of this paper. T_gs were recorded at the half-height of the corresponding heat capacity jumps, whereas the T_c, T_m and water thermodesorption temperatures were taken as the relevant peak temperatures. Heats of isolated peaks were computed by constructing linear baselines from the peak onset to completion and numerically integrated with appropriate software supplied by Mettler. For overlapping peaks, the baselines were constructed from the onset of the first peak to the completion of the second peak and the integration was carried out separately, below and above the valley between

Table 2
The hydration of PVP, PEG and their blends tested with DSC and DTG compared to the weight loss of specimens after scanning

Polymer	Sorbed water (wt%)		Weight loss (% after scanning)
	DSC	DTG	
PVP[a]	6.0	4.18	5.2
PVP–PEG (36 wt%)	7.3	7.78	8.1
PVP–PEG (69 wt%)	1.9	1.86	2.0
PEG	0.2	0.44	0.4

[a] As obtained from manufacturer. The hydration of PVP film dried from solution in ethyl alcohol vary from 10 to 12%.

the peaks. Due to dissimilarity in sample weights, the magnitudes of heat flow, presented in DSC traces throughout this work have been reduced everywhere to a reference weight of 10 mg.

3. Results and discussion

Characteristics of the phase transitions reported in this work relate to a scanning rate of 20°C min^{-1}. The majority of the transitions are heating-rate dependent and the rate effects upon T_g, T_c, T_m, ΔH_c, ΔH_m, and the temperature of water desorption, T_d, are displayed in Table 1. To generate the table, blends were heated at the rates of 10, 20, 30 and 40°C min^{-1}, and isothermal characteristics were estimated by extrapolating relevant linear relationships to zero rate. Linear regression parameters, R and p, show statistically insignificant rate-dependence for T_m, while the T_g, T_c, T_d, ΔH_c and ΔH_m-relationships are fairly fitted with linear graphs being plotted against both the rate of heating and the square root of this rate. The apparent T_m independence on heating rate is most likely due to dominant depression of blend crystallinity by hydration. T_m and the heat of water thermodesorption (ΔH_d) are much more affected by blend hydration than PEG content, as disclosed in the third article of this series. Reasons for the heating rate dependence of the area under the melting endotherm, ΔH_m, are considered in the second paper of this series. Measured at the heating rate of 20°C min^{-1} the T_g and T_c values are on average 4 and 6°C higher than their respective magnitudes found by extrapolation to zero rate. With the increasing PEG concentration the difference between measured and extrapolated T_g and T_m values tends to decrease. The ΔH_m and ΔH_c vary linearly with the content of crystalline PEG and deviations from this rule, displayed in Table 1, are caused by a hydration effect, as shown in the third paper.

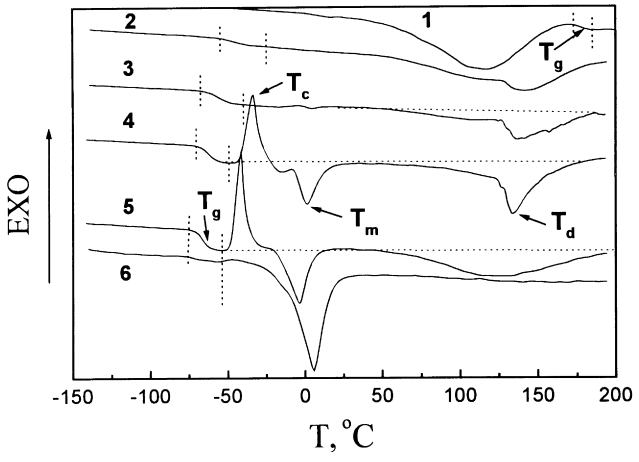

Fig. 1. DSC heating thermograms for PVP–PEG blends over the range of PEG/PVP compositions (in wt%): (1) 100% PVP; (2) 36% PEG; (3) 52.9% PEG; (4) 69.2% PEG; (5) 84.9% PEG; (6) 100% PEG. Storage time and conditions: three months at RH = 50%, 25°C.

The loss in weight of a specimen after thermal scanning is not always indicative of its hydration degree but may also be due to partial material decomposition at high temperatures. The DSC technique is reported to provide an alternative tool to determine the amount of water sorbed by hydrophilic polymers [36]. To accomplish this, the heat of water thermodesorption must match that of bulk water evaporation. Polymer hydration may then be measured through the enthalpy change associated with water desorption, dividing the obtained dehydration enthalpy by the reference value of water vaporization, $\Delta H = 2255$ J g^{-1}. This measurement is justified if specific water sorption in PVP–PEG hydrogels and polymer components does not contribute appreciably in the enthalpy of water thermodesorpion, i.e. the energy of water H-bonding to polymer units is comparable with the energy of H-bonds, formed between water molecules in clusters. To be certain of the validity of using the reference ΔH value, the amounts of water sorbed with PVP–PEG blends and initial polymers, as obtained from DSC heating thermograms, were compared to those measured by differential thermogravimetry (DTG) technique. The identical blends were simultaneously heated with a rate of 10°C min^{-1} from 25 to 200°C in the DSC apparatus and in a Mettler TG 50 DTG analyser. The results are presented in Table 2 along with the weight loss of specimens after scans. Both measurements give similar results, confirming the validity of using DSC for evaluation of water content in PVP and PVP–PEG blends. The relative inaccuracy of DSC technique in assessing water sorption with pure PEG is the result, most likely, of very low water sorption.

DSC traces for PVP, PEG and their blends are shown in Fig. 1. The scan of unblended PVP reveals a broad symmetric endotherm of water thermodesorption at 116°C

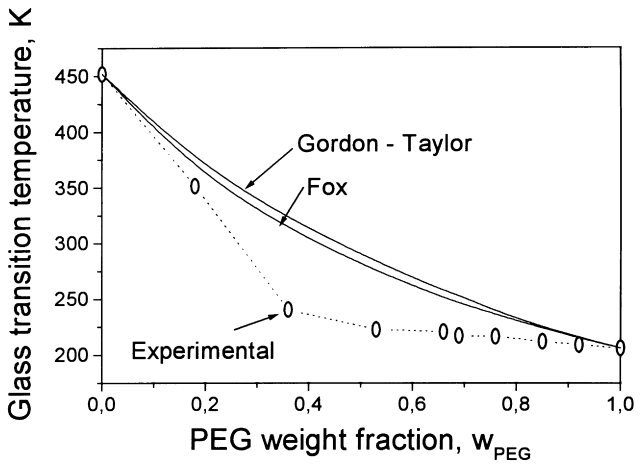

Fig. 2. The T_g of dry PVP–PEG blends as a function of PEG weight fraction. Points—experimental values, lines—the relationships described by the Fox and the Gordon–Taylor ($k = 0.55$) equations.

followed by a heat capacity jump at the glass transition ($T_g = 178°C$, $\Delta C_p = 0.27\ J\ g^{-1}\ K^{-1}$). The amount of water sorbed with PVP, determined as a ratio of water thermodesorption enthalpy to the reference value of bulk water vaporization heat, is found to be 7.3 wt%. This value is in close agreement with the loss in the sample weight after scanning (6.6 wt%). Immediate rescanning of the specimen using the same heating program shows neither endotherm nor weight loss, while the parameters of PVP glass transition remain practically intact. No freezing water is detected under PVP hydration even if 20% water sorption is attained.

The DSC heating curve of unblended PEG following its exposure to water vapour at RH = 50% (Fig. 1) displays glass transition at −70°C, $\Delta C_p = 0.32\ J\ g^{-1}\ K^{-1}$ and PEG fusion endotherm at $T_m = 6°C$, $\Delta H_m = 118.4\ J\ g^{-1}$. The PEG is nearly six times less hydrated than PVP, and the broad peak of water desorption is shifted to 127°C. As the content of sorbed water increases to 11.3%, ΔC_p achieves the value $1.17\ J\ g^{-1}\ K^{-1}$ and the glass transition in PEG becomes more conspicuous ($T_g = -71°C$). Again, no freezing water is found as the PEG hydration is so high as 17 wt%, corresponding to maximum bound water content reported to be 2.7 water molecules per PEG unit [37,38].

Since the PVP and PEG glass transition temperatures differ by a value of about 250°C, the peculiarities of T_g compositional behaviour in their blends are easily discernible (Fig. 1). A single composition dependent T_g, intermediate between those of the pure components, is an unambiguous criterion of the PVP–PEG compatibility. In the analysis of PVP–PEG miscibility, not only the number of glass transitions and their location on the temperature scale, but also their breadth were considered. Both the onset and endpoint of the glass transition in PVP–PEG compatible blends were recorded: the onset T_g was evaluated at the intersection of the pre-event baseline and a line drawn tangentially to the inflection point, while the endpoint was evaluated at the intersection of the inflection point tangent and the baseline established after the thermal event. A large transition width in PVP-overloaded blends, defined as the difference between the endpoint and onset T_gs and as a difference between inflection point and midpoint of glass transition, implies a broad spectrum of segment mobilities due to local heterogeneties caused by locally different degrees of PVP–PEG interaction. As PEG concentration in blend increases, both the cooperativeness of glass transition and ΔC_p become greater (Fig. 1).

Upon heating quench-cooled samples through T_g, the PVP-overloaded blends exhibit only the uppermost endotherms of water thermodesorption, while for PEG-overloaded mixtures the exotherms of PEG cold crystallization coupled with the PEG melting endotherms appear within intervening temperature ranges (Fig. 1). The water thermodesorption endotherms occur only in the scans of first heating and disappear at immediate rescanning. The enthalpy of water thermodesorption correlates with weight loss of the specimen after heating. (The effect of composition on this endotherm is considered in the third paper of this series.) By contrast, the enthalpies of the intervening exotherm and endotherm relate directly to PEG concentration in the blends and are only slightly affected by hydration. Although free water fusion in hydrogels occurs in the same temperature region, in PVP–PEG blends the thermal peaks characterize the PEG phase behaviour. Indeed, the peaks are equally inherent in both dry and hydrated blends, occurring both in the first and in the subsequent scans. These features argue unequivocally in favour of assigning the relevant peaks to excess PEG cold crystallization and fusion.

Since only the glass transition is featured without exception for all the dry and hydrated, amorphous and crystalline PVP–PEG blends, we start our analysis with the consideration of T_g compositional behaviour. While the scrutinity of cold crystallization–melting and vaporization peaks can be augmented to provide intrinsic information about the states of PEG and water in miscible blends, only the glass transition can be used to signify the mechanism of PVP–PEG interaction over entire composition range.

A variety of equations have been proposed to express the T_g-composition dependence in miscible polymer blends and plasticized systems, as reviewed by Aubin and Prud'homme [39]. In general, it is observed that T_g varies monotonically as a function of composition and the difference between measured T_g values and those predicted with relevant equations is usually considered as a measure of the strength of interactions between molecules of the involved components. When blends are formed from strongly interacting pairs, specific bonds bridge long sequences of repeat units of complementary chains, decreasing free volume between them and increasing packing density and the energy of cohesion. In full agreement with Eq. (6), the T_gs of the blends in this instance are generally much higher than the values calculated as weight averages of the component polymers. Large positive deviations of T_g values from those predicted with the Fox [40] and Gordon–Taylor [41]

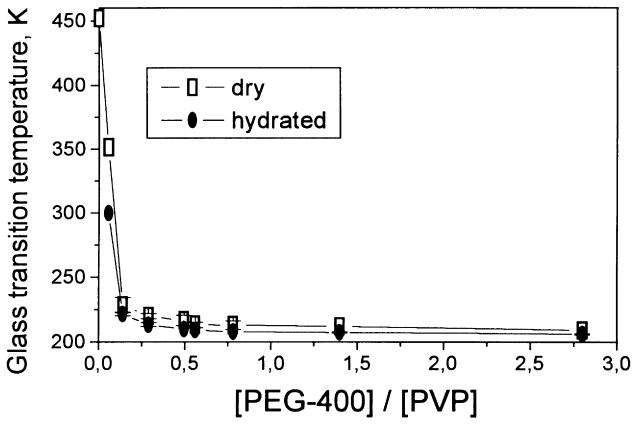

Fig. 3. The T_g of dry and freshly prepared (hydrated) PVP–PEG blends plotted against the number of PEG chains per one PVP unit available in the blend.

equations now appear to be a common occurrence in interpolymeric H-bonded and cation–anion complexes [42–45]. Large positive deviations are typical of PVP blends with hydroxyl-containing epoxy resin [46]. As regards to PVP H-bonded complexes with other hydroxyl containing polymers, such as polyvinyl alchohol [47,48], poly(hydroxyethyl methacrylate), poly(hydroxypropyl methacrylate) [49], and poly(*N*-phenyl-2-hydroxytrimethylene amine) [50], as well as for PVP miscible blends with polysulfone [51], poly(amide enaminonitile) [17], and phenoxy resin [52], the plots of T_g against the blend composition have been shown to follow fairly well the Fox, Gordon–Taylor, and Kwei [53] equations [47].

In contrast, H-bonding in PVP–PEG compatible blends results in large negative deviations from the simple rules of mixing expressed by the Fox and Gordon–Taylor equations (Fig. 2). With only 36 wt% of liquid PEG-400 added to glassy PVP, the blend T_g drops dramatically over 220°C, approaching the T_g value found for pure PEG. Following PVP mixing with plasticizer demonstrates a gradual levelling

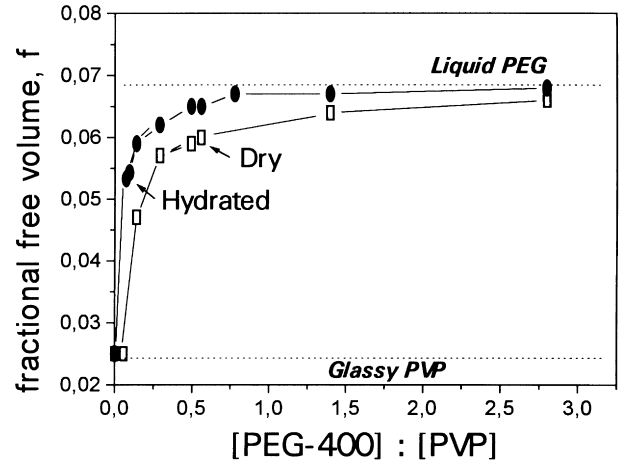

Fig. 4. The fractional free volume, *f*, calculated with Eq. (12) from T_g values, as a function of PVP–PEG blends composition at 20°C.

off the response in blend T_g (Figs. 2 and 3). Within the frameworks of the classical polymer plasticization–dissolution concept the first stage of the PVP–PEG mixing may be identified as PVP plasticization, whereas the second stage consists in gradual dissolution of the plasticized polymer in excess plasticizer [54]. The driving force for PEGs plasticizing action is the H-bonding of hydroxyl groups at the ends of PEG short chains to carbonyls in PVP repeat units as has been established with FTIR spectroscopy [23]. The first stage represents, therefore, PVP–PEG complexation and the boundary between the two stages (i.e. the blend containing 36 wt% of PEG-400) corresponds to a PVP–PEG stoichiometric complex [25]. Upon achieving this PEG concentration in blend, the exothermic heat of H-bonds formation ceases to dominate the unfavourable change in PVP–PEG noncombinatorial interaction entropy, which has been shown to be negative [25]. By H-bonding PVP units through terminal hydroxyl groups, the PEG short and flexible chains behave as spacers increasing the free volume between PVP neighbour segments. The T_g data in Figs. 2 and 3 enable in estimating the fraction of free volume, *f*, in PVP–PEG blends (Fig. 4) by the combination of the Doolittle and Williams–Landell–Ferry (WLF) equations [55]:

$$\frac{1}{2.303}\left(\frac{1}{f}-\frac{1}{f_g}\right)=-\frac{Nf_c}{2.303f_g}\,\frac{T-T_g}{(f_g/\Delta\alpha)+T-T_g}$$

$$=-\frac{17.37(T-T_g)}{51.6+T-T_g} \qquad (12)$$

where f_g is the fractional free volume of a polymer at T_g, $\Delta\alpha$ is the change of thermal expansion coefficient of polymer at T_g ($\Delta\alpha \approx 4.8\times10^{-4}\ K^{-1}$), f_c is the critical fractional free volume required so that a segment may jump or move and N the number of moving units per segment. As was shown by Bueche, $Nf_c \approx 1$, Fox and Flory found $f_g \approx 0.025$ for the majority of polymers [55]. Substitution of all the constants to Eq. (12) gives an expression ready to use.

The increase of free volume upon PVP–PEG mixing also appears from the compositional plot of another fundamental characteristic of glass transition, ΔC_p (Fig. 5). As Tanaka has shown [56]

$$\Delta C_p=\left(\frac{d}{dT}\left[\left\{RT^2\frac{d\ln Z(T)}{dT}\right\}/n\right]\right)_p$$

$$-\left(\frac{d}{dT}\left[RT^2\frac{d\ln V}{dT}\right]\right)_p+\left(\frac{dH_0}{dT}\right)_p+1.5R \qquad (13)$$

where $Z(T)$ is the steady-state conformational sum of a selected polymer chain at temperature T; V is the molar free volume per polymer segment; n the polymerization degree and H_0 the molecular cohesive energy per one mole of polymer segments. The drop in ΔC_p at small PEG concentrations (Fig. 5) is the result of the dominant free volume contribution that has been found to arise at

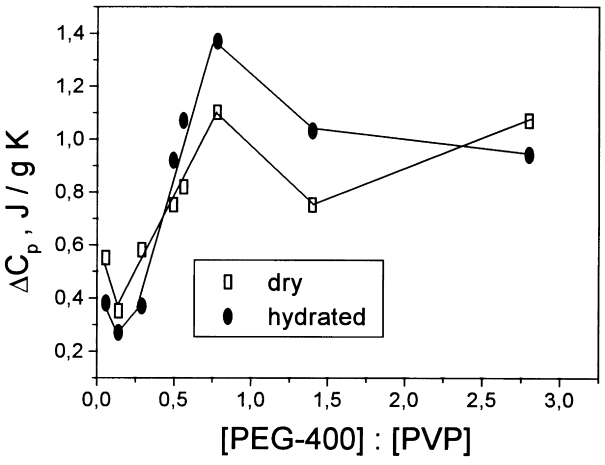

Fig. 5. The change in heat capacity, ΔC_p, between glassy and rubbery states plotted against the composition of freshly prepared and dry PVP–PEG blends.

PVP–PEG complex formation (Fig. 4). The subsequent growth in ΔC_p is most likely a consequence of enhancing the energy of intermolecular interaction and H-bonding between macromolecules as PEG content in the blend increases. At minimum ΔC_p the energy of intermolecular cohesion within the PVP–PEG blend is specifically balanced by the fluctuation free volume. The observed reduction in ΔC_p for PEG-overloaded blends (Fig. 5) is due to their high crystallinity degree. It is known that ΔC_p tends to decrease as crystallinity increases.

Although the T_g values of dry PVP–PEG blends are found to be somewhat higher than those for hydrated blends (Fig. 3), the sorbed water does not reveal itself as a compatibilizer in PVP–PEG system, because both dry and hydrated blends are compatible, demonstrating only one composition-dependent glass transition. This conclusion is presented in more quantitative terms in the third paper of this series.

Coherent behaviour of T_g, T_m and T_c in PVP–PEG

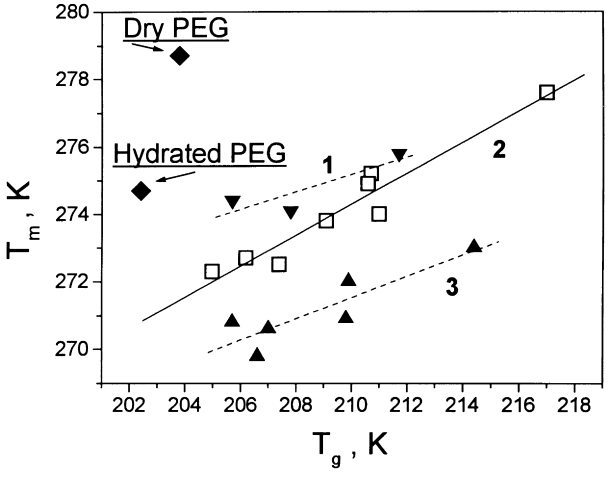

Fig. 6. Effects of PVP–PEG blend composition and storage conditions on the relationship between glass transition and PEG melting temperatures: (1) aged blends; (2) RH = 50%; (3) freshly prepared blends.

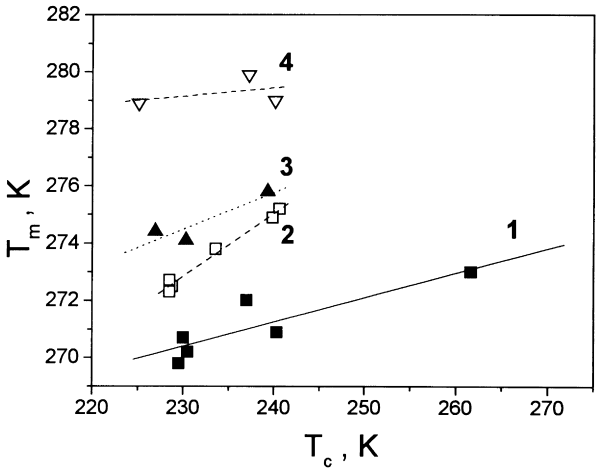

Fig. 7. Effects of PVP–PEG blend composition and storage conditions on the relationship between PEG cold crystallization and melting temperatures upon heating quench-cooled samples through glass transition: (1) fresh blends; (2) RH = 50%; (3) February; (4) May.

compatible blends is illustrated in Figs. 6 and 7. In agreement with the rules outlined by Eqs. (1) and (2), T_m is a linear function of T_g and T_c, however depending on the time and conditions of storage, the samples of different prehistory are characterized with noticeably different slopes and intercepts ($R = 0.88$–0.99). Thus, freshly prepared blends exhibit lower T_m values, but after being set aside for a period of up to one year, the blends show signs of long-term evolution or "ageing", which among other changes result in the increase in melting temperature. The melting temperature is affected by the perfection of the crystal structure and, consequently, structural relaxation processes underlie the accompanying changes with time in the phase transition temperatures of PVP–PEG blends.

In freshly prepared blends, produced by evaporation of common solvent at ambient temperatures, the PEG chains, attached to PVP units through H-bonding of terminal hydroxyls, are most likely randomly disordered in their positions along PVP chains. The self-assembly of several PEG chains into energetically more favourable ordered structures is supposed to be a driving force for the observed ageing. Similar self-assembly of ionic surfactant amphiphilic molecules into clusters is reported to accompany surfactant binding with oppositely charged polyelectrolytes [57]. The PEG chains orientation within such ordered structures has been recently shown by WAXS study of PVP–PEG blends to match closely that of PEG crystals [23]. It is obvious that the more the PEG chains being assembled into crystal-like structures, the higher the T_m. On the other hand, sorbed water is capable of disrupting crystal perfection and depressing T_m. Aged blends are appreciably drier than freshly prepared ones and exhibit higher T_ms. The changes in blend hydration account for seasonal effects observed in phase behaviour of aged PVP–PEG blends. The blends tested in February after nine months of storage at comparatively lower RH are referred throughout

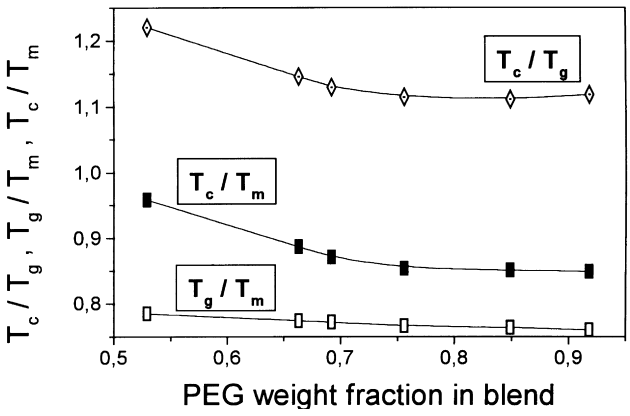

Fig. 8. The T_g/T_m, T_c/T_g and T_c/T_m quantities as the functions of PEG concentration in freshly prepared blends.

this work to as "February", whereas those tested in May following the storage for a period of one year at higher RH of surrounding atmosphere are designated as "May" or simply "aged" blends. The analysis of seasonal effects is presented in the third paper of this series, in which the impact of hydration upon phase behaviour has been shown to dominate over the influence of storage time. For the purposes of the present discussion, the data sets obtained for different storage conditions are considered separately in relation to PEG content in blends, thereby minimising the effects of relative humidity.

Fig. 8 illustrates the dependence of T_g/T_m, T_c/T_g and T_c/T_m quantities on the composition of freshly prepared PVP–PEG blends. These are explicit functions of blend composition, expressed in terms of PEG weight fraction. Being reduced to the most basic molecular level, the temperatures of phase transitions are interrelated through the structure of the polymer. In compatible polymer blends the phase behaviour results from polymer mixing at a molecular level and varies in accord with composition. As PEG concentration in the blend increases, the T_g/T_m value varies linearly from

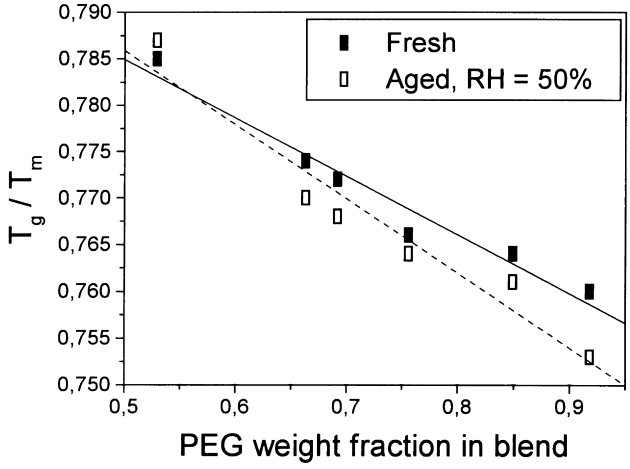

Fig. 9. Effect of storage conditions on the compositional behaviour of T_g/T_m quantity in PVP–PEG compatible blends, freshly prepared and aged for three months at RH = 50% and 25°C.

0.785 to 0.760, whereas other quantities decrease smoothly from $T_c/T_m = 0.958$ to 0.849 and from $T_c/T_g = 1.220$ to 1.111. Compared with reference average magnitudes found for a variety of individual polymers (Eqs. (1)–(3)) [1], in PVP–PEG blends the T_g/T_m and T_c/T_m values are at the upper edges of the relevant ranges, while the T_c/T_g value is at the lower boundary. It should be emphasized that the obtained values relating to the PEG cold crystallization peak temperatures upon heating quench cooled samples from glassy state, T_c, match closely the reference magnitudes obtained after cooling polymers from the melt. This finding implies that in PVP–PEG compatible blends the maximum cold crystallization rate temperature is in close agreement with the temperature of maximum crystallization rate. Since the quantity $(1 - T_g/T_m)$ defines the fraction of full free volume required to provide polymer transition from the glassy into the rubbery state and the transition from crystalline phase to melt [12], comparatively enlarged T_g/T_m values in PVP–PEG blends imply facilitated PVP–PEG complex devitrification and PEG fusion. This finding is thoroughly explicable using the concept of fluctuation free volume formation under PVP–PEG mixing (Fig. 4). Being enriched with the fluctuation free volume, the PVP–PEG blends need less additional free volume for polymer transition into the viscoelastic state and for fusion.

While the T_g/T_m quantity varies linearly with blend composition, all the T_c-dependent quantities display the deviations from linearity at comparatively low PEG concentrations (Fig. 8). This fact is due to the contribution of molecular mobility to the T_c value as shown in the second paper of this series and illustrated below by the data in Fig. 13. The levelling off the response at high PEG weight fractions ($w_{PEG} > 0.8$) for T_c/T_m and T_c/T_g plots (Fig. 8) results most likely from the disentanglement of PVP chains and gel–solution transition. Using optical microinterference measurements of the kinetics of high molecular weight PVP dissolution in liquid PEG-400, the PVP transition from swollen gel into solution has been recently found to occur at $w_{PEG} > 0.8$.

Dependence of T_g/T_m quantity on PEG weight fraction in freshly prepared and stored blends with PVP is shown to obey the following equations:

$$\frac{T_g}{T_m} = 0.82 - 0.06 w_{PEG};$$

$R = -0.98$, $p = 0.0006$ (fresh blends)

$$\frac{T_g}{T_m} = 0.83 - 0.08 w_{PEG}; R = -0.97,$$

$p = 0.0013$ (after blend exposure to water vapour for three months at RH = 50% and 25°C)

$$\frac{T_g}{T_m} = 0.90 - 0.17 w_{PEG}; \; R = -0.99,$$

$p = 0.017$ (dry blends)

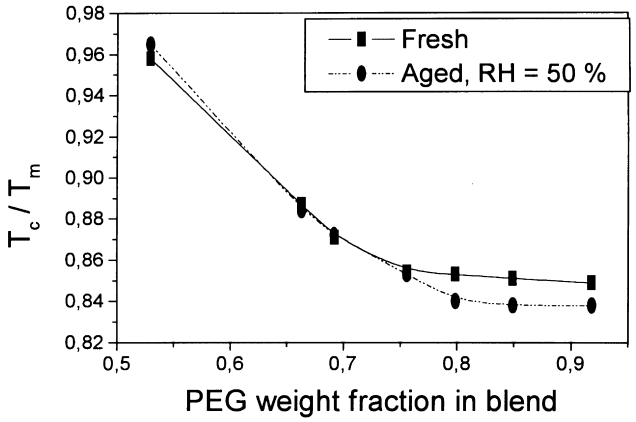

Fig. 10. Dependence of T_c/T_m quantity on the PEG content in PVP–PEG blends freshly prepared and exposed to water vapour for three months at RH = 50% and 25°C.

The storage conditions' effect on the T_g/T_m and T_c/T_m quantities are presented in Figs. 9 and 10. Providing appreciable contribution to phase behaviour, those nevertheless are not decisive for PVP–PEG compatibility and for interrelationships between phase transition temperatures.

The overall relationship between all the three transition temperatures in PVP–PEG compatible blends is given in Fig. 11. In the view of Eq. (9), the plot is indicative of the compositional behaviour of the α_g/α_c ratio in PVP–PEG blends. With the rise in PEG concentration, the α_g/α_c ratio increases linearly until a critical PEG concentration of $w_{PEG} = 0.8$ is attained. Since only PEG is capable of forming a crystalline phase in PVP–PEG mixtures, the thermal expansion coefficient of crystalline polymer, α_c, is a characteristic of PEG and is supposed to be approximately invariant with PEG content. Consequently, the increase in the α_g/α_c ratio with PEG weight fraction embeds, most likely, the increasing thermal expansion coefficient of PVP–PEG complex in glassy state, α_g.

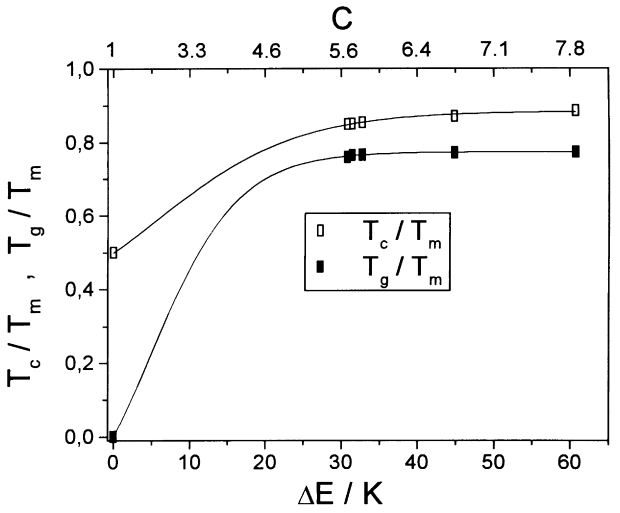

Fig. 12. The Okui plot of T_c/T_m and T_g/T_m quantities in PVP–PEG blends of various prehistory, obtained with Eqs. (7)–(10).

Analysis of the T_g/T_m and T_c/T_m quantities for PVP–PEG compatible blends in terms of an Okui iso-volume state model and crystallization theory [1], featuring the activation energy of polymer segment migration through nucleus–melt interface, ΔE, nucleation parameter, K, and a constant, C, defined by Eqs. (10) and (11), is presented in Fig. 12. The greater the C and $\Delta E/K$ values the greater the T_g/T_m and T_c/T_m quantities, however the large variations in C and $\Delta E/K$ in the region of their upper values cause relatively negligible changes in the T_g/T_m and T_c/T_m, as seen in Fig. 12. Apart from the minimum magnitudes of $C = 1$ and $\Delta E = 0$, determined by definition (10), all the data points relating to the PVP–PEG blends fall in the region $C > 5.5$ and $\Delta E/K > 29$. With increasing PEG content, the $\Delta E/K$ gradually increases, tending to values as high as $\Delta E/K = 525$ at minimum PEG concentration when crystallization occurs ($w_{PEG} = 0.53$, Fig. 13). For individual homopolymers

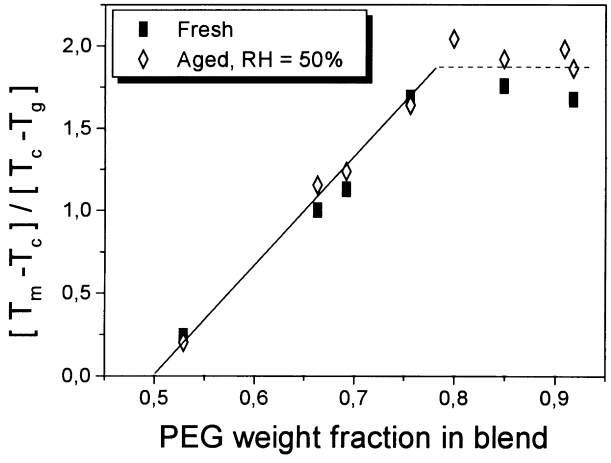

Fig. 11. The ratio of $T_m - T_g$ and $T_c - T_g$ differences plotted against PEG concentration in blends with PVP.

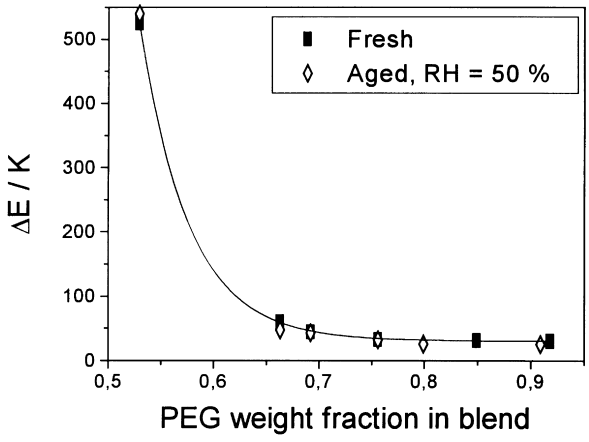

Fig. 13. The dependence of $\Delta E/K$ quantity, determined with Eqs. (10) and (11), on the PEG weight fraction in compatible blend with PVP.

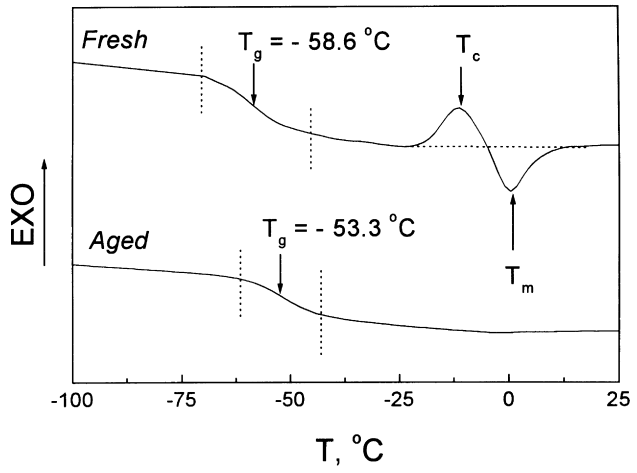

Fig. 14. DSC traces upon heating of freshly prepared and aged PVP blends containing 52.9 wt% of PEG-400.

C has been found to vary from 3 to 9, corresponding to the change in $\Delta E/K$ value between 8 and 80. The average value of $\Delta E/K$ is about 23 ($C \approx 4.9$) in most polymers [1].

Abnormally high $\Delta E/K$ values for PEG-underloaded blends, ($w_{PEG} < 0.53$), give a plausible explanation for the lack of any crystallization and fusion processes observed in DSC heating traces of relevant mixtures (Fig. 1). It seems reasonable to say that the $\Delta E/K \approx 500$–600 defines an upper limit of the range of activation energy, providing the existence of freezing PEG in the blends with PVP. As liquid PEG is added to glassy PVP, the blend T_g falls abruptly (Figs. 2 and 3). No crystalline phase is observed at the stage of PVP–PEG complexation (plasticization) (Fig. 2), while the T_g exceeds some critical magnitude. Upon the reduction of T_g value below this critical magnitude, the PEG crystallization becomes allowable. As is evident from Fig. 13, Eqs. (7), (8) and (10), comparatively negligible variations in T_g/T_m value within this critical region are due to dramatic changes in $\Delta E/K$, which enable or prohibit the crystalline phase formation.

This conjecture is conveniently illustrated in Fig. 14. In freshly prepared blends containing 52.9 wt% of PEG-400 and characterized with $T_g = 214.4$ K, both PEG crystallization and fusion occurs upon sample heating through T_g ($T_c = 261.6$ K, $T_m = 273$ K, $T_g/T_m = 0.785$, $\Delta E/K = 526$). As the same blend is allowed to relax for nine months at ambient temperatures and relative humidities, the T_g increases by as little as 5.3 K, and the freezing PEG ceases to be detected. The contribution of molecular mobility to the PEG crystallization in compatible blends with PVP is discussed in more detail in the second article of this series.

4. Conclusions

DSC heating traces of cool-quenched PVP–PEG compatible blends reveal a single, composition-dependent glass transition, intermediate between those of unblended polymer components, along with the phase transitions of excess PEG cold crystallization and melting, followed by the uppermost endotherm of sorbed water vaporization. In the compatible blends all the temperatures of phase transitions, as well as the T_g/T_m, T_c/T_m and T_c/T_g quantities, are shown to be functions of the composition. Extremely large negative deviations from simple rules of mixing, expressed by the Fox and Gordon–Taylor equations, in the T_g dependence on the composition are due to the earlier reported H-bonding of short-chain PEG terminal hydroxyl groups to carbonyls in the repeating units of PVP macromolecules, accompanied by free volume formation. The antagonistic contributions to the glass transition of conflicting strong favourable interaction between macromolecules of blended polymers and the free volume within PVP–PEG complex are embedded by a specific profile of the compositional dependence of a heat capacity change between the glassy and viscoelastic states, ΔC_p. Occurrence of a crystalline phase in the compatible PVP–PEG blends is controlled by the molecular mobility of the crystallizable polymer.

Acknowledgements

This research was in part made possible by Award No. RN2-409 of the US Civilian Research & Development Foundation for the Independent States of the Former Soviet Union (CRDF). We express our appreciation to Professors Ronald A. Siegel, Anatoly E. Chalykh, Yuly K. Godovsky, Michael M. Coleman and Paul C. Painter for their helpful discussion and comments.

References

[1] Okui N. Relationships between melting temperature, maximum crystallization temperature and glass transition temperature. Polymer 1990;31(1):92–4.
[2] Boyer RF. The relation of transition temperatures to chemical structure in high polymers. Rub Chem Technol (Rub Rev) 1963;36(5):1303–421.
[3] Beamen RG. Relation between (apparent) second-order transition temperatures and melting point. J Polym Sci 1952;9:470–2.
[4] Lee WA, Knight GJ. Ratio of the glass transition temperature to the melting point in polymers. Brit Polym J 1970;2(1):73–8.
[5] Van Krevelen DW. Properties of polymers. 3. Amsterdam: Elsevier, 1990 chaps. 4, 16 and 19.
[6] Mandelkern L. Crystallization of polymers. New York: McGraw-Hill, 1964.
[7] Godovskii YK. Effect of temperature and structure of macromolecules on polymer crystallization rate. Polym Sci USSR 1969;10:2129–34.
[8] Privalko VP. Universal relation for polymer crystallization rates from the melt. Polymer 1978;19(9):1019–25.
[9] Utracki LAJ. Temperature dependence of liquid viscosity. Macromol Sci, Phys B 1974;10(3):477–505.
[10] Askadskii AA, Matveev YuI. Chemical structure and physical properties of polymers. Moscow: Chemistry, 1983 p. 24–48.
[11] Camello Ph, Lazzeri V, Walyell B, Cypcar Ch, Mathias LJ. Glass

transition temperature calculations for styrene derivatives using the energy, volume and mass model. Macromolecules 1998;31(11): 2305–11.
[12] Askadskii AA. Structure-property relationships in polymers: quantitative analysis. Polym Sci, Ser B 1995;37(2):332–57.
[13] Paul DR, Newman S. Polymer blends. New York: Academic Press, 1978.
[14] Coleman MM, Graf JF, Painter PC. Specific interactions and the miscibility of polymer blends. Lancaster, PA: Technomic, 1991.
[15] Coleman MM, Narvet LA, Painter PC. A counterintuitive observation concerning hydrogen bonding in polymer blends. Polymer 1998;39(23):5867–9.
[16] Lee NY, Painter PC, Coleman MM. Hydrogen bonding in polymer blends. 4. Blends involving polymers containing methacrylic acid and vinylpyridine groups. Macromolecules 1988;21(4):954–9.
[17] Moore JA, Kaur S. Blends of poly(amide-enaminonitrile) with poly-(ethylene oxide), poly(4-vinylpyridine), and poly(*N*-vinylpyrrolidone). Macromolecules 1998;31:328–35.
[18] Kirsh YE. Water soluble poly(*N*-vinylamides). New York: Wiley, 1998.
[19] Sakellariou P, Abraham MH, Whiting GS. Solubility characteristics of poly(ethylene oxide): effect of molecular weight, end groups, and temperature. Colloid Polym Sci 1994;272(7):872–5.
[20] Cesteros LC, Quintana JR, Fernandez JA, Katime IA. Miscibility of poly(ethylene oxide) with poly(*N*-vinyl pyrrolidone): DMTA and DTA studies. J Polym Sci, Polym Phys Ed 1989;27:2567–76.
[21] Papisov IM, Baranovsky VY, Sergieva EI, Antipina AD, Kabanov VA. Thermodynamics of poly(methacrylic) and poly(acrylic) acids complexation with poly(ethylene glycols). Polym Sci USSR Ser A 1974;16:1133–41.
[22] Buehler V. Kollidon: polyvinylpyrrolidone for the pharmaceutical industry. 3. Ludwigshafen: BASF, 1996;19–20.
[23] Feldstein MM, Lebedeva TL, Shandryuk GA, Kotomin SV, Kuptsov SA, Igonin VE, Grokhovskaya TE, Kulichikhin VG. Complex formation in poly(*N*-vinyl pyrrolidone-poly(ethylene glycol) blends. Polym Sci 1999;41(8):854–66.
[24] Lebedeva TL, Igonin VE, Feldstein MM, Platé NA. H-bonding poly-(ethylene glycol) to poly(*N*-vinyl pyrrolidone) within an adhesive hydrogel matrix for transdermal drug delivery. Proc Int Symp Controlled Release Bioact Mater 1997;24:447–8.
[25] Feldstein MM, Shandryuk GA. Quantitative relation of glass transition temperature to polymer–plasticizer binding degree. Proc Int Symp Controlled Release Bioact Mater 1999;26:1084–5.
[26] Bairamov DF, Feldstein MM, Chalykh AE. In preparation.
[27] Feldstein MM, Shandryuk GA, Kuptsov SA. In preparation.
[28] Feldstein MM, Lebedeva TL, Shandryuk GA, Igonin VE, Avdeev NN, Kulichikhin VG. Stoichiometry of poly(*N*-vinyl pyrrolidone)-poly(ethylene glycol) complex. Polym Sci 1999;41(8):867–75.
[29] Dormidontova E, ten Brinke G. Phase behaviour of hydrogen-bonding polymer–oligomer mixtures. Macromolecules 1998;31(8):2649–60.
[30] Ruokolainen J, ten Brinke G, Ikkada O, Torkkeli M, Serimaa R. Mesomorphic structures in flexible polymer–surfactant systems due to hydrogen bonding. Macromolecules 1996;29(10):3409–15.
[31] Kotomin SV, Borodulina TA, Feldstein MM, Kulichikhin VG. Sqeeze–recoil analysis of adhesive hydrogels and elastomers. Polym Mater Sci Engng 1999;81:425–6.
[32] Chalykh AA, Chalykh AE, Feldstein MM. Effects of composition and hydration on adhesive properties of poly(*N*-vinyl pyrrolidone)-poly-(ethylene glycol) hydrogels. Polym Mater Sci Engng 1999;81:427–8.
[33] Chalykh AE, Chalykh AA, Feldstein MM. Fracture mechanics of poly(*N*-vinyl pyrrolidone)-poly(ethylene glycol) hydrogel adhesive joints. Polym Mater Sci Engng 1999;81:427–8.
[34] Feldstein MM, Chalykh AE, Chalykh AA, Platé NA. Quantitative relationship between molecular structure and adhesion of PVP–PEG hydrogels. Polym Mater Sci Engng 1999;81:465–6.
[35] Chalykh AE, Chalykh AA, Feldstein MM, Siegel RA. Isotherms of water sorption with the blends of poly(*N*-vinyl pyrrolidone)-poly-(ethylene glycol). Proc Int Symp Controlled Release Bioact Mater 1999;26:393–4.
[36] Zang YH, Sapiecha S. A differential scanning calorimetric characterization of the sorption and desorption of water in cellulose/linear low-density polyethylene composites. Polymer 1991;32(3):489–92.
[37] Hager SL, Macrury TB. Investigation of phase behaviour and water binding in poly(alkylene oxide) solutions. J Appl Polym Sci 1980;25:1559–71.
[38] Graham NB, Zulfigar M, Nwachuku NE, Rashid A. Interaction of poly(ethylene oxide) with solvenrs. 4. Interaction of water with poly-(ethylene oxide) crosslinked hydrogels. Polymer 1990;31(5): 909–16.
[39] Aubin M, Prud'homme RE. Analysis of the glass transition temperature of miscible polymer blends. Macromolecules 1988;21:2945–9.
[40] Fox TG. Influence of diluent and copolymer composition on the glass transition temperature of a polymer system. Bull Am Phys Soc 1956;1:123.
[41] Gordon M, Taylor JS. Ideal copolymers and the second-order transitions of synthetic rubbers. I. Non-crystalline copolymers. J Appl Chem 1952;2:493–500.
[42] Suzuki T, Pearce EM, Kwei TK. Hydrogen-bonded polymer complexes. Polymer 1992;33(1):198–201.
[43] Cowie JMG, Reilly AAN. Enhancement of miscibility in blends of poly(vinyl methyl ether) and poly(α-methylstyrene)s modified by incorporation of hydrogen-bonding sites. Polymer 1992;33(22): 4814–20.
[44] Coleman MM, Moscala EJ. FT IR studies of polymer blends containing poly(hydroxy ether of bisphenol A) and poly(ϵ-caprolactone). Polymer 1983;24(3):251–7.
[45] Hugglin MB, Rego JM. Study of polymer blends based on poly-(vinylpyridines) and acidic polymers. Polymer 1990;31(7):1269–76.
[46] Janarthanan V, Thyagarajan G. Miscibility studies in blends of poly(*N*-vinyl pyrrolidone) and poly(methyl methacrylate) with epoxy resin: a comparison. Polymer 1992;33(17):3593–7.
[47] Nishio Y, Haratani T, Takahashi T. Miscibility and orientation behaviour of poly(vinyl alchohol)/poly(vinyl pyrrolidone) blends. J Polym Sci, Polym Phys Ed 1990;28:355–74.
[48] Ping Z, Nguyen QT, Neel J. Investigation of poly(vinyl alchohol)/poly(*N*-vinyl-2-pyrrolidone blends. 1. Compatibility. Makromol Chem 1988;189:437–48.
[49] Goh SH, Siow KS. Miscible blends of poly(*N*-vinyl pyrrolidone) with some hydroxyl-containing polymers. Polym Bull 1990;23:205–9.
[50] Zhong Z, Mi Y. Thermal characterization and solid-state ^{13}C-NMR Investigation of blends of poly(*N*-phenyl-2-hydroxytrimethylene amine) and poly(*N*-vinyl pyrrolidone). J Polym Sci, Polym Phys 1999;37(2):237–45.
[51] Shult KA, Paul DR. Water sorption and transport in blends of poly-(vinyl pyrrolidone) and poly(sulfone). J Polym Sci, Polym Phys Ed 1997;35(4):655–74.
[52] Tsang CJ, Clark JC, Wellinghoff ST, Miller WG. Structure–property relationships in poly(*n*-vinyl pyrrolidone)-phenoxy–water gels. J Polym Sci, Polym Phys 1991;29(2):247–59.
[53] Kwei TK. The effect of hydrogen bonding on the glass transition temperatures of polymer mixtures. J Polym Sci, Polym Lett 1984;22(6):307–13.
[54] Feldstein MM. A two-stage mechanism of poly(*N*-vinyl pyrrolidone) mixing with short-chain poly(ethylene glycol). Proc Int Symp Controlled Release Bioact Mater 1998;25:848–9.
[55] Ferry JD. Viscoelastic properties of polymers. 2. New York: Wiley, 1970 chap. 11.
[56] Tanaka N. Conformational effects on glass transition temperature and relaxation phenomena of polymers. Polymer 1978;19(7):770–2.
[57] Feldstein MM, Zezin AB, Kabanov VA. The conformations of synthetic polypeptides in complexes with ionic surfactants. Mol Biol USSR 1974;8(2):218–26.